Journal of Applied Fluid Mechanics, Vol. 10, No. 3, pp. 861-870, 2017.
Available online at www.jafmonline.net, ISSN 1735-3572, EISSN 1735-3645.
DOI: 10.18869/acadpub.jafm.73.240.26527

Numerical and Experimental Investigation of Wiper System Performance at High Speeds

S. Cadirci[1†], S. E. Ak[1], B. Selenbas[2] and H. Gunes[1]

[1] *Department of Mechanical Engineering, Istanbul Technical University, Istanbul, 34437, Turkey*
[2] *Teklas Kaucuk A.S., Kocaeli, 41400, Turkey*

†*Corresponding Author Email: cadircis@itu.edu.tr*

(Received May 9, 2015; accepted January 8, 2017)

ABSTRACT

In this study, aerodynamic forces acting on the windshield wiper system at critical wiper angles are simulated using different wiper blade geometries, i.e., wiper and spoiler modifications, to solve the wiping problem occurring at high speeds due to lifting forces. Undesired aerodynamic lift forces reach a peak at critical blade angles, thus turbulent air flow around the wiper blades at critical angles on a car model is investigated numerically in detail to solve this problem. Previous experimental studies have shown that the front windshield wiper blades can be lifted up by aerodynamic forces between wiper blade angles of 30-40°, if no geometric modifications are done to prevent this. The possible modifications which can have a positive effect on wiper's performance include wiper's profile (also spoiler's curvature), wiper's height and connection type of the rubber part to the metal part. Aerodynamic lift and drag forces acting on the wiper blade and wiper arm are calculated for both driver's and passenger's sides. It is revealed that for both wiper blades on the driver's and passenger's sides, an increased wiper height with a blunt connection type can supply most satisfactory results in terms of decreased lift forces, in other words negative lift forces. Utilizing the output of the numerical analysis, the new wiper-blade-spoiler profile is selected and then manufactured to test its wiping performance in a thermal wind tunnel by soiling tests. Numerical studies are validated by experimental tests, since the new wiper profile has been proven as a more efficient prototype in terms of wiping performance compared to the original one.

Keywords: Wiper Blade; Aerodynamic Lift, Aerodynamic Drag; Computational Fluid Dynamics.

NOMENCLATURE

C_D	drag coefficient	α	inclination angle of the windshield
C_L	lift coefficient	ε	energy dissipation
F_X	calculated force in x direction	ρ	density of the fluid
F_Y	calculated force in y direction	μ	laminar viscosity
F_{Drag}	drag force	μ_t	turbulent (eddy) viscosity
F_{Lift}	lift force	σ_k	turbulent Prandtl number for k
k	turbulent kinetic energy	σ_ε	turbulent Prandtl number for ε
u_j	velocity vector		

1. INTRODUCTION

Windshield wiper systems are one of the important components in vehicle safety equipment. A conventional wiping system consists of three components, namely: motor mechanism, wiper arm and wiper blade. To wipe water and dirt from the front windshield, the wiper blade should be pressed to the windshield by a specified force at around 10 N. With the increasing vehicle speed, the down force decreases due to aerodynamic lift forces acting on wiper arm and wiper blade. To eliminate high lift forces acting on the wiper arms, adequate downward force is needed to press the wiper arm on the windshield by the wiper blade. Current standard flat blade (beam blade) wipers can work up to vehicle speeds around 160 km/h without apparent problems, however at relatively higher speeds such as 240 km/h, lift forces acting on the wiper blades become more dominant and this reduces the wiping quality. Most of the unwiped regions appear in the center of the flat blade wiper indicating that the lift forces are most effective in the center of the wipers. In the last decades, some researchers investigated aerodynamic lift acting on windshield wiper blades to improve the wiping

performance of a vehicle moving at a high speed. Clarke *et al*. (1960) studied the aerodynamic forces acting on windshield wiper system. They stated wiping quality decreases with increasing vehicle velocity. They carried out wind tunnel experiments for both on flat plate and a half car model and investigated the wiping quality up to speed of 140 km/h. They recommended using an airfoil could reduce lifting forces acting on wiper blade.

Dawley *et al*. (1965) investigated aerodynamic behavior of different vehicle parts, including the windshield wiper system. They gathered force data from wind tunnel experiments for a conventional type of wiper blade having an airfoil. They investigated the effect of airfoil's angle of incidence over lift force and concluded that with increasing angle of incidence, lift forces acting on the wiper blade could be reduced and after some point a down force could be achieved.

Jallet *et al*. (2001) carried out both experimental and numerical studies on windshield wiper blades. They used a horizontal flat surface in their calculations. For the conventional type of wiper blade they found 4.4 N of lift force at a speed of 144 km/h and 4 N of down force if the wiper blade has a spoiler. They used k-ε turbulence model in their numerical studies and validated their results by experiments.

Billot *et al*. (2001) continued the previous numerical study of Jallet *et al*., and investigated both conventional type of wiper blades and a new type of flat wiper blades on a car geometry. Both wiper blades were positioned in the mid-wipe position. For a speed of 160 km/h they calculated 9.8 N of lift force for the conventional type of wiper blade without a spoiler and 7.4 N of lift force for the wiper blade with the spoiler. For the new flat blade design, they found 4.9 N lift force.

Gaylard *et al*. (2006) studied the aerodynamic performance of beam type of wiper blades in a Sport Utility Vehicle at different wiping angles both numerically and experimentally. They were interested in the effect of the wiper components on the flow over the windshield. Their study provided a description of the flow and vortex structures associated with wiper systems.

Yang *et al*. (2011) numerically studied the aerodynamics around flat blade wipers on a car geometry. They used seven different wiping angles varying between 0° to 90° with an increment of 15° and carried out simulations at three vehicle speeds which are 30, 50 and 70 km/h. They found out that most aerodynamic lift forces were effective at angles between 30° and 45° on the driver's side and most critical angle was found to be 30° on the passenger's side.

Lee *et al*. (2009) did numerical investigation on the flat blade wipers on a half car model at high velocities. They used four wiping angles and two vehicle velocities such as 170 and 200 km/h. They found out that most aerodynamic lift force occurred on driver's side at half of the total wiping angle and at quarter of the total wiping angle on the passenger's side.

The current study is based on numerical findings by Cadirci *et al* (2016-a). Like this previous study, this current study emphasizes the advantages of creating useful wiper modifications and combining them to a useful prototype to achieve sufficiently down forces at high speeds and overcome undesired lift forces on wipers.

2. WIPER CONFIGURATION

2.1 Geometry of the Wiper Prototypes

The wiper configuration of interest is shown in Fig. 1. To investigate the effects of aerodynamic forces, four different modifications are suggested which can be seen in Fig. 2. Based on previous numerical studies related to the performance improvement of the flat blade wiper, three modifications have been suggested which are showed in Fig. 1. The main goal here is to generate down forces on the wipers. Model-0 is the original geometry which can be identified as standard flat blade wiper's geometry. Modifications are carried out on this original geometry and their effects are investigated including spoiler profile, wiper height and the connection type between wiper metal and the spoiler. A reasonable modified spoiler profile is designed to prevent vortex formation above the spoiler since much more pressure can be generated with this modification (Model-1). On the other hand, it was thought that the spoiler height might also have an effect on the down forces; as a result, Model-2 is dealing with this goal and it has succeeded in generating more down forces on the wiper blades. Finally, to get rid of the vortex formation between the metal part and the spoiler, a new modification is suggested such as Model-3. The modifications are summarized in Table 1.

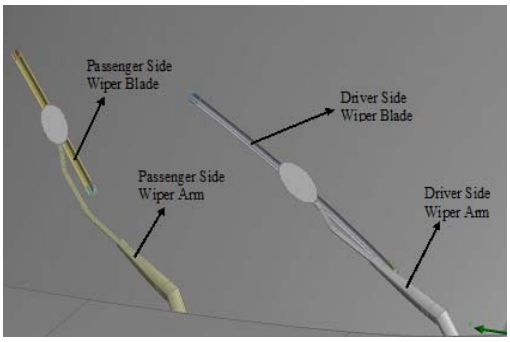

Fig. 1. Wiper system's configuration.

Table 1 Wiper modifications

Wiper Model	Spoiler Profile	Height [mm]	Connection Type
Model-0	Original	16.6	Original
Model-1	Modified	16.6	Original
Model-2	Modified	19.0	Original
Model-3	Modified	19.0	Modified

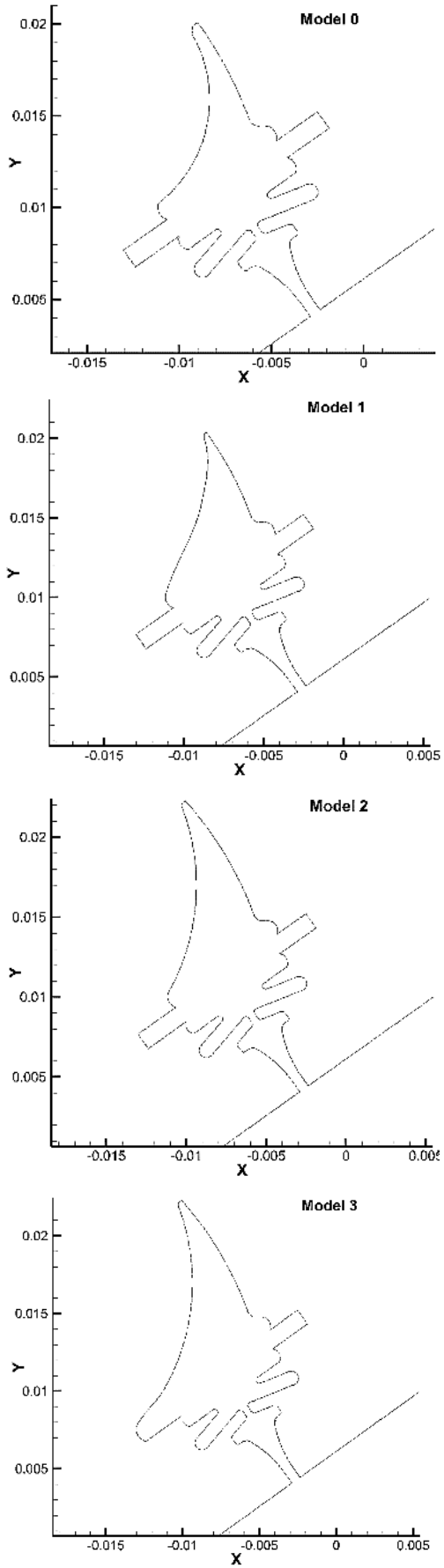

Fig. 2. Original and suggested wiper profiles, both axis are given in [m].

3. COMPUTATIONAL APROACHES

3.1 Computational Domain and Boundary Conditions

The 3-D domain of interest consists of a half car model, wiper blades and wiper arms for both on driver's and passenger's sides. The half car model is especially convenient to model flow around the windshield and wiper blades since the flow downstream of the vehicle are not of interest. The wiper blade on the driver side has a length of 600 mm and makes an angle of 30° with the horizontal plane. The wiper blade on the passenger side has a length of 450 mm and makes an angle of 45° with the horizontal plane as displayed in Fig.1. The half car model has a length (L) of 2570 mm, width (W) 1560 mm and height (H) 970 mm. The 3-D computational domain around the half car model and wiper blades is designed sufficiently large and has the dimensions 5L x 5W x 5H to obtain reliable computational results.

Figure 3 shows the computational domain with the imposed boundary conditions. On the inlet control surface of the domain, velocity inlet boundary condition is imposed with appropriate turbulence intensity. The velocity profile is assumed to be uniform and is set equal to 240 km/h for all simulations, since the most undesired aerodynamic lift-up effects occur at such high speeds.

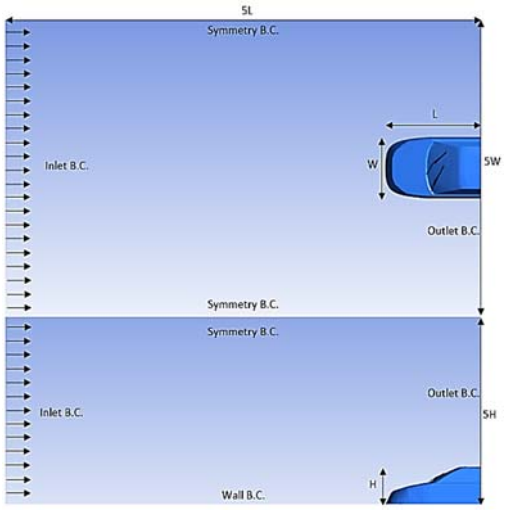

Fig. 3. Solid model of the domain and imposed boundary conditions for the half-car model.

On the outlet control surface, downstream of the half car model, outlet boundary condition is specified. The surface of the car, wiper arms and the road have no-slip boundary conditions with enhanced wall functions. The remaining surfaces of the domain are specified with symmetry boundary conditions.

To indicate that the computational results are independent of the grid size, three different dense meshes are created for Model-0. These grids have 20, 45 and 60 million tetrahedral elements as tabulated in Tab.2. Tetrahedral elements are then converted to polyhedral elements to reduce the total number of

elements, for instance the grid with 45 million tetrahedral elements is reduced to a grid with 13 million polyhedral elements. The mesh is densely clustered in the vicinity of the wiper system and car surface in the boundary layer regions.

Details of the mesh selected to be used in the simulations can be seen as a slice through the entire computational domain in Fig.4; as a close-up-view in the vicinity of the wiper arm and blade on driver's side in Fig.5 and for both wiper arms on the driver's and passenger's sides in Fig.6.

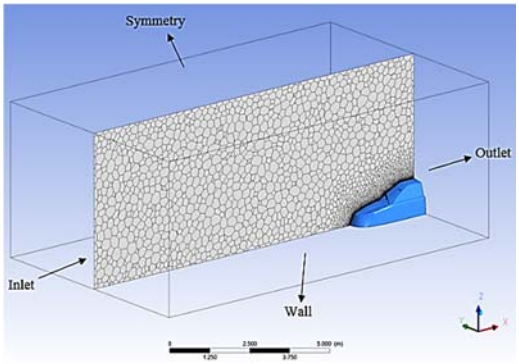

Fig. 4. Mesh-slice through the 3-D computational domain.

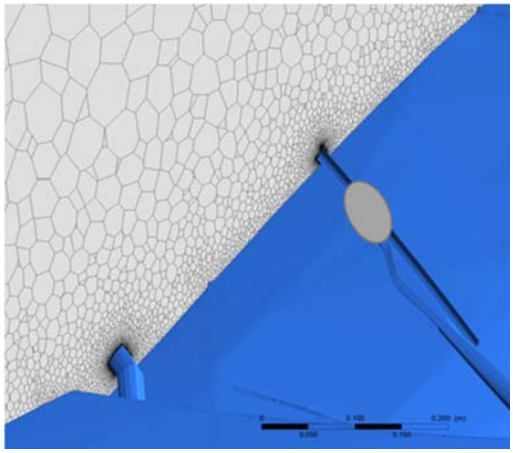

Fig. 5. Wiper blade and wiper arm on driver's side with a mesh-slice.

3.2 Computational Settings and Governing Equations

The flow is simulated by a finite-volume-based flow solver (ANSYS-Fluent). Working fluid is air and the flow is steady, incompressible and turbulent. The realizable *k-ε* turbulence model with enhanced wall functions is preferred among possible *k-ε* turbulence models as proposed by Cadirci et.al. (2016-b), since realizable *k-ε* turbulence model is capable of modeling aerodynamics with high reliability. The SIMPLE algorithm is used with second order upwind schemes for momentum and transport equations of turbulence kinetic energy and turbulence kinetic energy dissipation. The turbulent length scale is assumed to be the height of the spoiler which is either 16.6 mm or 19 mm. The turbulence intensity level at the inlet is set equal to 3%. The thermo-physical properties of the fluid are constant. The density is ρ=1.225 kg/m^3 and the laminar viscosity is μ=1.79 x 10^{-5} kg/ms.

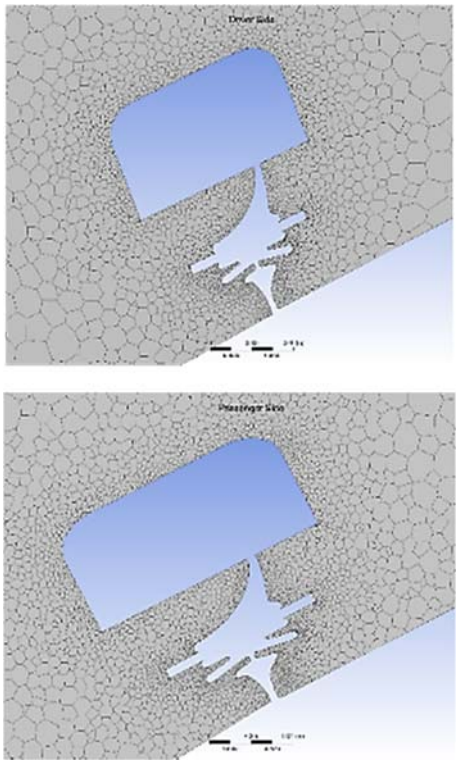

Fig. 6. Selected mesh with nearly 13 million polyhedral elements: Left: driver's side, right: passenger's side.

The conservation equations for the problem are continuity and incompressible, steady, turbulent Navier-Stokes equations. The transport equations of the turbulent kinetic energy and of turbulent kinetic energy dissipation are given in Eq. (1) and (2) respectively. Turbulent viscosity and the model constants used in the transport equations for the realizable *k-ε* turbulence model are indicated in Eq. (3) based on ANSYS Fluent Theory Guide (2013).

$$\frac{\partial}{\partial t}(\rho k)+\frac{\partial}{\partial x_j}(\rho k u_j)=\frac{\partial}{\partial x_j}\left[\left(\mu+\frac{\mu_t}{\sigma_k}\right)\frac{\partial k}{\partial x_j}\right] \quad (1)$$
$$+G_k+G_b-\rho\varepsilon-Y_M+S_k$$

$$\frac{\partial}{\partial t}(\rho \varepsilon)+\frac{\partial}{\partial x_j}(\rho \varepsilon u_j)=\frac{\partial}{\partial x_j}\left[\left(\mu+\frac{\mu_t}{\sigma_\varepsilon}\right)\frac{\partial \varepsilon}{\partial x_j}\right]$$
$$+\rho C_1 S\varepsilon-\rho C_2\frac{\varepsilon^2}{k+\sqrt{\nu\varepsilon}}+C_{1\varepsilon}\frac{\varepsilon}{k}C_{3\varepsilon}G_b+S_\varepsilon \quad (2)$$

In Eq. (1) and (2), G_k represents the generation of turbulence kinetic energy due to mean velocity gradients and G_b is the generation of turbulence kinetic energy due to buoyancy. In Eq.(3) μ_t is the turbulent viscosity and S is the mean rate of strain tensor.

Table 2 Mesh independence tests for Model-0

No of elements [Million]	Side	Part	F_{Drag} [N]	F_{Lift} [N]	ΣF_{Lift} [N]	C_D	C_L
20	Drv.	Blade	15.3	-1.1	3.7	0.592	-0.043
		Arm	10.7	4.8		0.469	0.212
	Pas.	Blade	5.5	-0.41	0	0.368	-0.027
		Arm	3.8	0.38		0.169	0.024
45	Drv.	Blade	15	-1.07	3.7	0.58	-0.041
		Arm	10.7	4.75		0.471	0.209
	Pas.	Blade	5.4	-0.26	0.1	0.363	-0.018
		Arm	3.9	0.38		0.173	0.017
60	Drv.	Blade	14.9	-1.1	3.6	0.578	-0.041
		Arm	10.7	4.7		0.472	0.205
	Pas.	Blade	5.4	-0.19	0.2	0.361	-0.013
		Arm	3.7	0.35		0.165	0.015

$$\mu_t = \rho C_\mu \frac{k^2}{\varepsilon}$$
$$C_1 = max\left[0.43, \frac{\eta}{\eta+5}\right] \quad (3)$$
$$\eta = S\frac{k}{\varepsilon} \quad S = \sqrt{2S_{ij}S_{ij}} \quad S_{ij} = \frac{1}{2}\left(\frac{\partial u_j}{\partial x_i} + \frac{\partial u_i}{\partial x_j}\right)$$
$$C_{1\varepsilon} = 1.44 \quad C_2 = 1.9 \quad \sigma_k = 1.0 \quad \sigma_\varepsilon = 1.2$$

3.3 Calculation of Aerodynamic Forces

For all calculations, drag and lift forces acting on the wiper and spoiler are calculated as indicated in Fig.7 where F_X and F_Y are obtained from numerical calculations. Depending on the inclination angle of the windshield (α) lift and drag forces can be found by using Eq. 4 and their corresponding coefficients can be calculated by using Eq. 5 where U stands for free stream velocity and A_p for the projection area of the wiper blade.

$$F_{Lift} = F_Y \cos\alpha - F_x \sin\alpha$$
$$F_{Drag} = F_Y \sin\alpha + F_x \cos\alpha \quad (4)$$

$$C_L = \frac{F_{Lift}}{\frac{1}{2}\rho U^2 A_p} \quad ; C_D = \frac{F_{Drag}}{\frac{1}{2}\rho U^2 A_p} \quad (5)$$

3.4 Computational Results

The wiping performances of the modified wiper prototypes are tested at a free stream velocity of U = 240 km/h. As one can see from Table 3, the total lift force acting on the original blade geometry is calculated 3.7 N on the driver's side and 0.1 N on the passenger's side. A modified wiper (Model-1) has a new spoiler design which can reduce the total lift force by nearly 1.0 N as indicated in Table 3. Further wiper blades of 19 mm height (Model-2) and blunt connection type (Model-3) can supply more satisfactory results in terms of total lift coefficient reduction since down force can be achieved on the wiper system. The main goal of the study is to generate down forces to overcome lifting at high speeds, nevertheless the analysis results reveal that with increased spoiler height much more drag forces occur on the wiper blades.

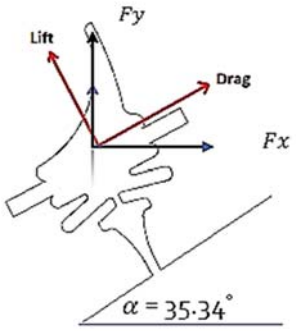

Fig. 7. Aerodynamic forces acting on windshield wiper.

To show pressure distributions on the wiper blades, 2D slices are extracted excluding wiper arms. As one can see in Fig. 8, modified wiper prototypes (Model-1-2 and-3) have increased pressure distributions on their spoilers both on driver's and passenger's sides compared to the original wiper.

Additionally, iso-surfaces are obtained using λ_2 (Lamdba-2) vortex determination criterion. These vortices in flow field obtained by λ_2 methodology reveal detailed flow structures. There are several vortex identification methods, one of them is λ_2 vortex identification as investigated by Jeong *et al.* (1995). λ_2 vortex criterion is a detection algorithm that can adequately identify vortices from a three-dimensional velocity field. It consists of several

Table 3 Comparison of aerodynamic characteristics of proposed wiper modifications

Model	Side	Part	F_{Drag} [N]	F_{Lift} [N]	ΣF_{Lift} [N]	C_D	C_L
0	Drv.	Blade	15	-1.1	3.7	0.58	-0.041
		Arm	10.7	4.7		0.471	0.209
	Pas.	Blade	5.4	-0.26	0.1	0.363	-0.018
		Arm	3.9	0.38		0.173	0.017
1	Drv.	Blade	14.9	-2.2	2.3	0.575	-0.085
		Arm	10.6	4.5		0.468	0.2
	Pas.	Blade	5.7	-0.2	0.5	0.379	-0.013
		Arm	3.8	0.68		0.17	0.03
2	Drv.	Blade	18.3	-5.1	-0.7	0.708	-0.199
		Arm	10.5	4.5		0.461	0.196
	Pas.	Blade	6.7	-1.29	-0.9	0.447	-0.086
		Arm	3.7	0.34		0.162	0.015
3	Drv.	Blade	18.7	-5.9	-1.1	0.726	-0.227
		Arm	10.6	4.74		0.465	0.209
	Pas.	Blade	6.6	-1.45	-1.0	0.444	-0.097
		Arm	3.7	0.49		0.164	0.022

steps: first the velocity gradient tensor is defined and then the tensor is decomposed into its symmetric and antisymmetric parts, both parts are obtained by the velocity tensor and its transpose. Next for each point in the velocity field three eigenvalues are calculated and ordered in descending order. A point in the velocity field is part of a vortex core only if at least two of its eigenvalues are negative, or $\lambda_2 < 0$.

In Fig. 9a, modified wiper prototypes such as Model-2 and Model-3 with a larger wiper height can elongate the vortex structures more than Model-0 (given in Fig.9b in close-up) and Model-1 especially on the driver's side of the vehicle. On the driver's side vortices occur directly behind the wiper arm and blade where on the passenger's side the vortices form nearly at the tip of the wiper blade.

4. EXPERIMENTS

4.1 Wind Tunnel Facility

To reveal the performance of the developed wiper-spoiler prototype supplying best aerodynamic performance in terms of reduced lift forces, soiling tests have been carried out in a thermal wind tunnel. To obtain more reliable experimental results, the spring pre-load is initially measured by a force-meter (10.7 N) before applying aerodynamic forces in the wind tunnel. In the experiments water droplets with fluorescent agent are added to the air flow and made visible using UV-light. Automatic evaluation and qualification of the resulting soiling are done afterwards. The specifications of the thermal wind tunnel are as follows:

a) A test section of 15.8 m x 6.8 m x 5.5 m

b) Air jet velocity 240 km/h for smaller jets (4 m^2).

c) Operating temperature between 20-50°C

Figures 10a-d show instantaneous snapshots captured during soiling tests at various speeds for the original and modified wiper prototype. The snapshots are selected in a way that the wiper blades are located at the possible lowest positions to reveal one wiping cycle in one wiping period. The velocity of the air flow varies between 180 and 240 km/h. The usage of the modified wiper prototype is found to be satisfactory since the water spots on the windshield disappear especially at high speeds. The undesired water spots occurring on the windshield with the original wiper on the driver's side are indicated in red dotted circles.

It can be noted in Figs. 10a-c that the original wiper blade's performance is insufficient in preventing the occurrence of water spots even at velocities lower than 240 km/h. The experiments proved the advantage of the new proposed wiper-blade-design at the free stream velocity of 240 km/h, since the large water spot on the driver's side is avoided to a large extent.

5. CONCLUSIONS

Since the wiper system is vital for both driver's and passenger's safety at bad-weather conditions, the wiper blade should be designed in a way to prevent undesired lift-up forces occurring at high vehicle speeds. In this study, aerodynamic forces acting on the wiper arms and blades for different modified

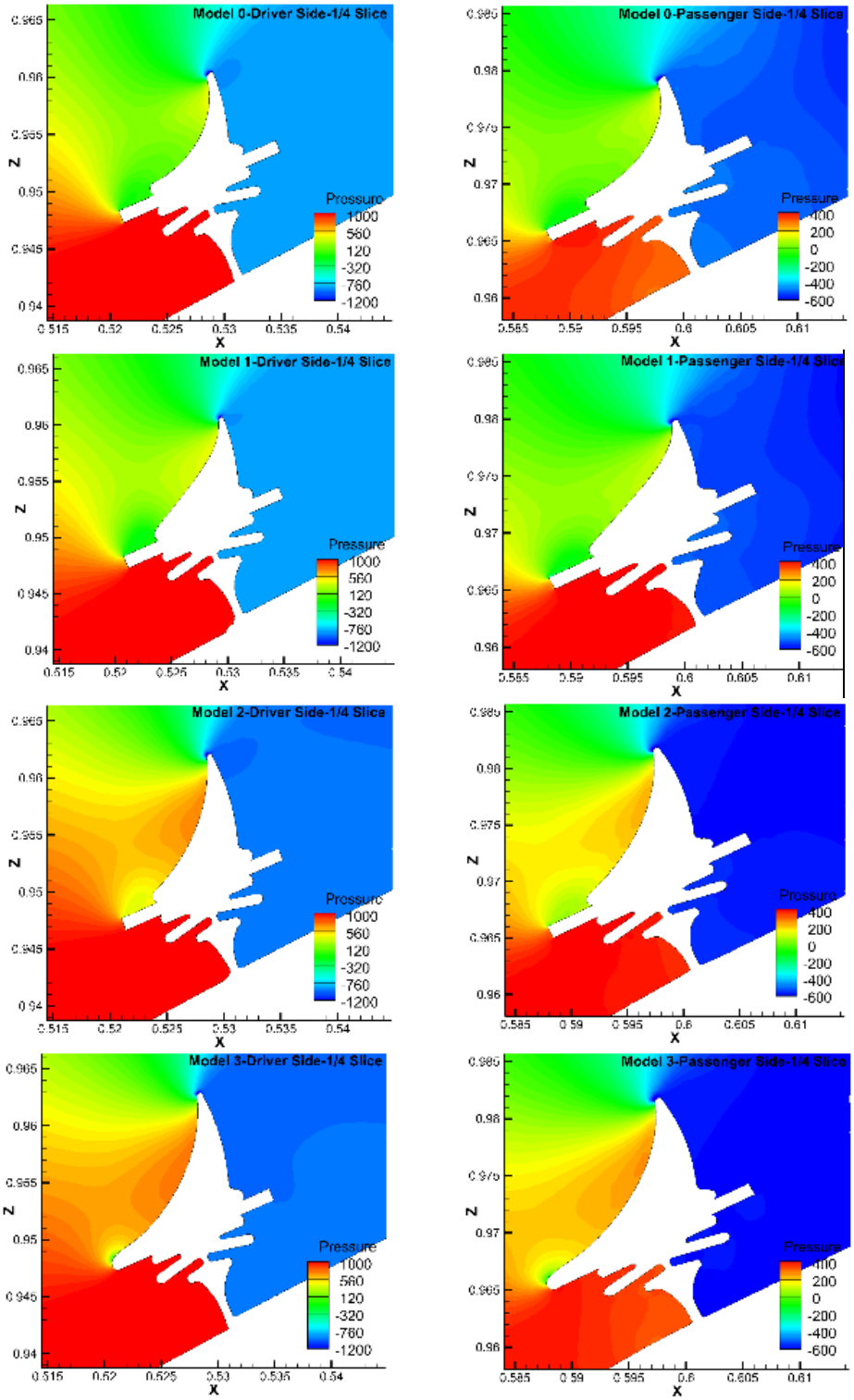

Fig. 8. Pressure distributions in [Pa] for Models-0-1-2-and -3; left column is driver's side, right column is passenger' side; both-axis are given in[m].

prototypes are investigated computationally. The simulations are carried out by a finite-volume based steady, turbulent, incompressible flow solver at a free stream velocity of 240 km/h.

The effects of three geometric parameters of the wiper are investigated in detail: wiper-spoiler's profile, wiper's height and the connection type. All of the proposed modifications result in more satisfactory wiping performances compared to the original wiper design. The computational results are evaluated according to the total lift coefficients calculated on the wiper arms and blades both on driver's and passenger's sides.

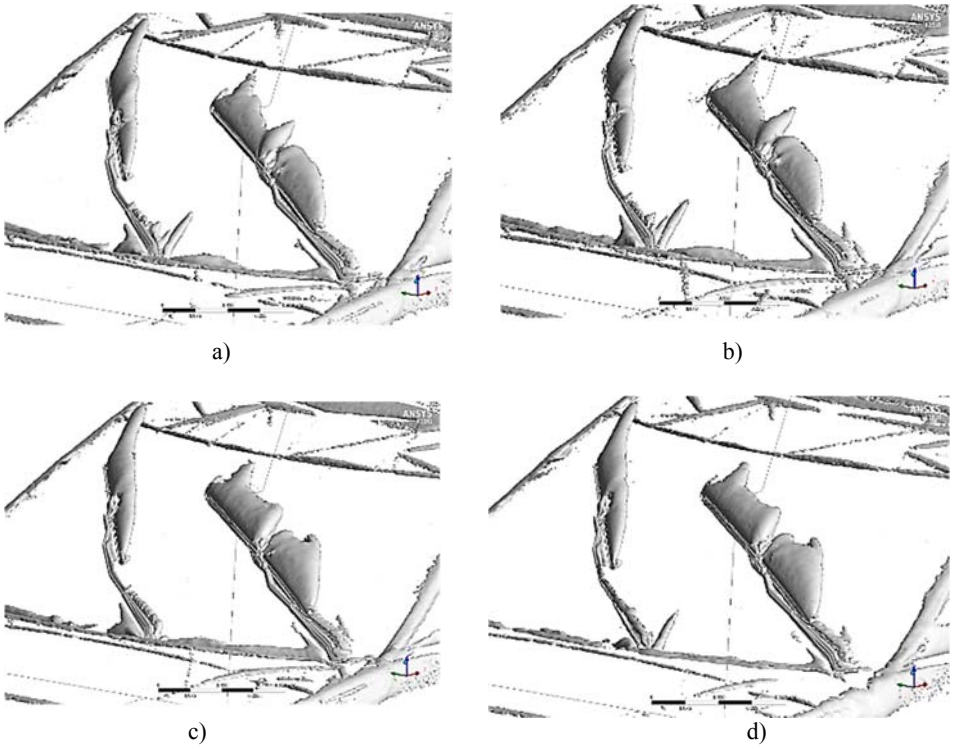

Fig. 9a. Iso-surfaces from λ_2 vortex determenitaion (level=0.001) for (a) Model-0, (b) Model-1, (c) Model-2, (d) Model-3.

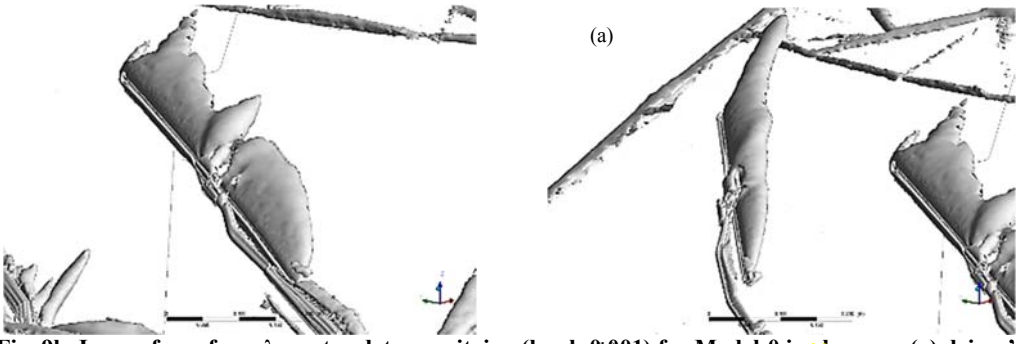

Fig. 9b. Iso-surfaces from λ_2 vortex determenitaion (level=0.001) for Model-0 in close-up: (a) driver's side, (b) passenger's side.

The wiper arm and blade are investigated separately with the purpose of predicting the down forces separately. Changing the spoiler's curvature (profile) and wiper's height assist the wiper to overcome undesired lift forces by increasing the pressure distribution along the upper surface of the spoiler. It is revealed that an increased wiper's height with a blunt connection type can supply most satisfactory results in terms of better wiping performance since sufficient down force can be achieved to press the wiper onto the windshield. Furthermore, λ_2-vortex-identification criterion reveals that by modifying the wiper design, more elongated vortex structures can occur which can affect the lift forces considerably.

Computational results are then validated by soiling tests carried out in a thermal wind tunnel at various free-stream velocities. It is shown qualitatively that the proposed wiper design can avoid the water spots on the windshield on the driver's side. The predicted wiping performance of the new wiper design from numerical simulations is observed by soiling tests experimentally. It is believed that this study fills an important gap in the field of wiper-design aiming an efficient and satisfactory wiping performance at high speeds.

ACKNOWLEDGEMENTS

The authors are indebted to Ministry of Science, Industry and Technology of Turkey and Teklas Kaucuk A.S. for financial support through the project 0278-STZ-2013-2. Furthermore, the authors are thankful to Forschungsinstitut für Kraftfahrwesen und Fahrzeugmotoren (FKFS) at the University Stuttgart, Germany for giving us the permission to use their thermal wind tunnel.

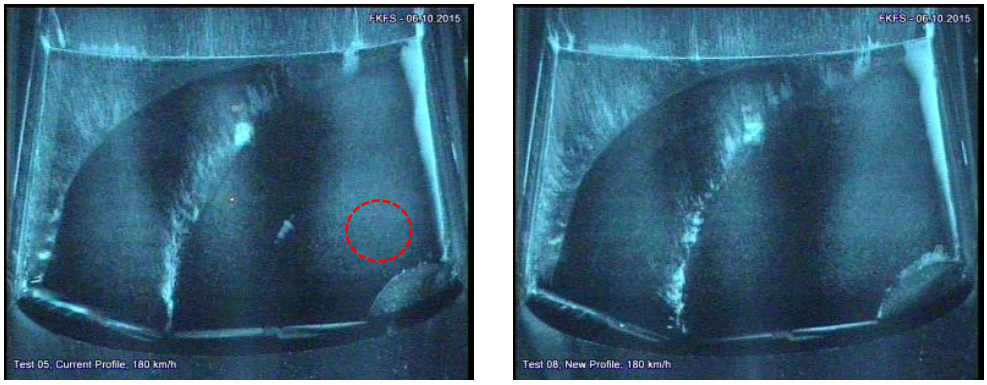

(a) U = 180 km/h

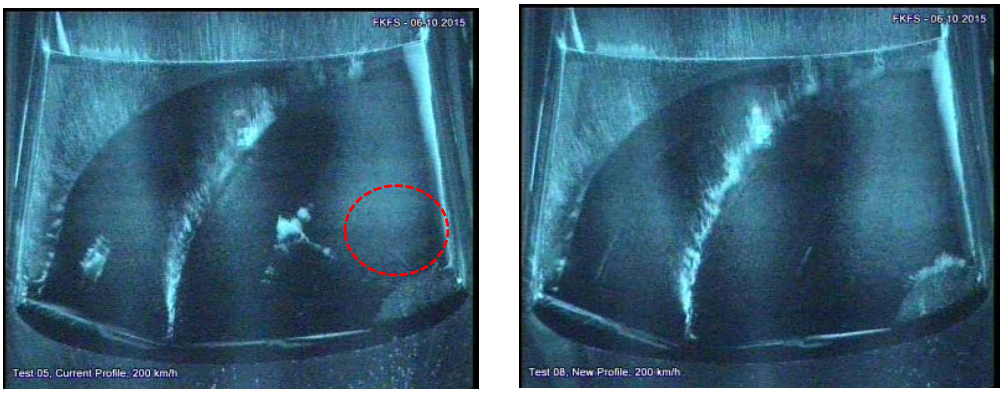

(b) U = 200 km/h

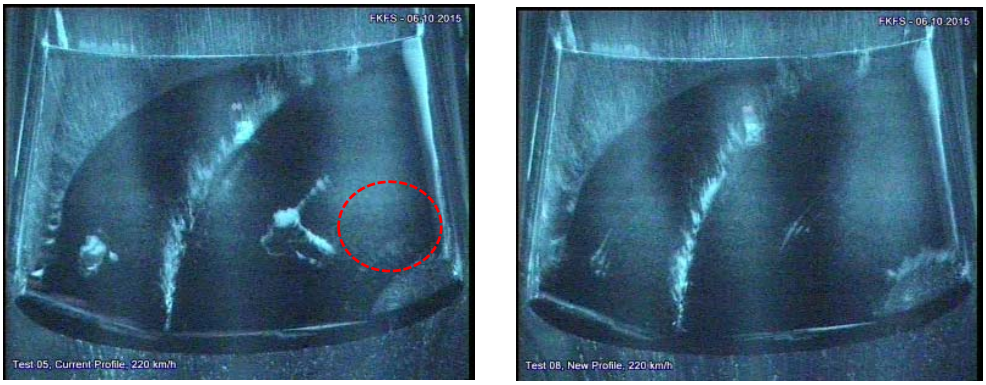

(c) U = 220 km/h

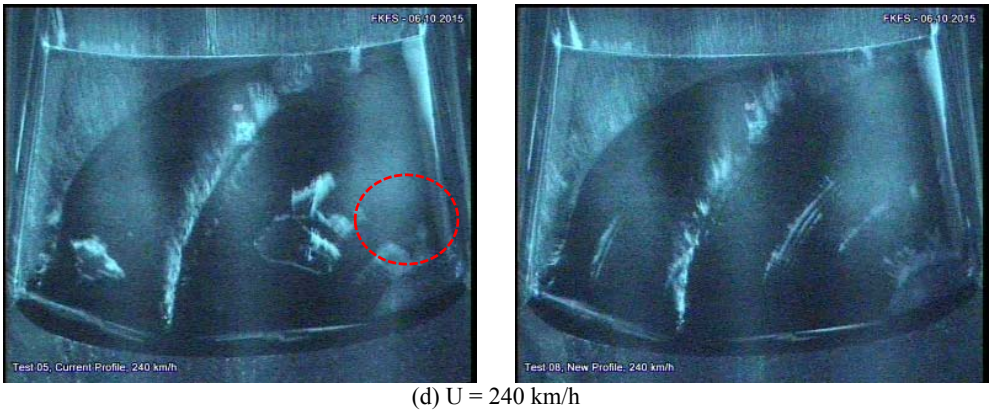

(d) U = 240 km/h

Fig. 10. Captures from wiping tests when wiperblades are at lowest position; left columns are for the original wiper, right columns for the modified wiper.

REFERENCES

ANSYS Fluent Theory Guide Release 15 (2013). 51-54.

Billot, P., S. Jallet and F. Marmonier (2001). Simulation of Aerodynamic Uplift Consequences on Pressure Repartition - Application on an Innovative Wiper Blade Design. *SAE Technical* 01-1043.

Cadirci, S., S. E. Ak, B. Selenbas and H. Gunes (2016-a). Geometric Modifications to Minimize Lift Acting on a Simplified Front Windshield Wiper Blade. *Journal of Thermal Science and Technology* 36(2), 103-109.

Cadirci, S. and *et al.* (2016-b). Numerical Investigation of Turbulent Flow over a Windscreen Wiper Blade. In *ASME-International Mechanical Engineering Congress and Exposition*.

Clarke, J. and R. Lumley (1960). Problems Associated with Windscreen Wiping. *SAE Technical Paper*.

Dawley, M. (1965). Aerodynamic Effects on Automotive Components. *SAE Technical Paper*.

Gaylard A. P., A. C. Wilson and G. S. J. Bambrook (2006). A Quasi-Unsteady Description of Windscreen Wiper Induced Flow Structures. In *6th MIRA International Vehicle Aerodynamics Conference*.

Jallet, S. and *et al*. (2001). Numerical Simulation of Wiper System Aerodynamic Behavior. *SAE Technical Paper*.

Jeong, J. and F. Hussain (1995). On the identification of a vortex. *Journal of Fluid Mechanics* 285, 69-94.

Lee, S. H. and *et al.* (2009). Numerical Study on the Aerodynamic Lift on the Windshield Wiper of High-Speed Passenger Vehicles, In *The Proceedings of Asian Symposium on Computational Heat Transfer and Fluid Flow* 3, 185-190.

Yang, Z. G., X. M. Ju and Q. L. Li (2011). Numerical Analysis on Aerodynamic Forces on Wiper System. *Proceedings of the Sixth International Conference on Fluid Mechanics*, AIP Proceedings 1376, 213-217.